

2023-03-21

Organic Solvent Free Synthesis and Processing of Semiconducting Polymers for Field Effect Transistors in Waterborne Dispersions

Chiara Ceriani, Mattia Scagliotti, Tommaso Losi, Alessandro Luzio, Sara Mattiello, Mauro Sassi, Nicolò Pianta, Matteo Rapisarda, Luigi Mariucci, Mario Caironi, Luca Beverina

Wiley-VCH

Chiara Ceriani, Mattia Scagliotti, Tommaso Losi, Alessandro Luzio, Sara Mattiello, et al.

2023. Organic Solvent Free Synthesis and Processing of Semiconducting Polymers for Field Effect Transistors in Waterborne Dispersions. *Advanced Electronic Materials* 9(5). doi: <https://doi.org/10.1002/aelm.2>

<https://open.uns.ac.rs/handle/123456789/32636>

Downloaded from DSpace-CRIS - University of Novi Sad

Organic Solvent Free Synthesis and Processing of Semiconducting Polymers for Field Effect Transistors in Waterborne Dispersions

Chiara Ceriani, Mattia Scagliotti, Tommaso Losi, Alessandro Luzio, Sara Mattiello, Mauro Sassi, Nicolò Pianta, Matteo Rapisarda,* Luigi Mariucci, Mario Caironi,* and Luca Beverina*

Conjugated semiconducting polymers are key active materials for printable electronics, sensors and biosensors, organic photovoltaics, organic light emitting devices, and more. The research in the field developed very efficient materials and sound structure property relationships, thus making a case for a transition from laboratory to industrial environment. At this critical juncture, sustainability, and ease of scaling up are at least as important as performances, to the point that efficient materials on a lab scale could become unpractical for the industry. The development of more efficient synthetic protocols and the complete removal of all organic solvents from both the synthesis and the processing of semiconducting polymers can help tremendously to improve sustainability and reduce costs. It is shown that the use of an aqueous dispersion of the food grade surfactant lecithin as the medium, enables the synthesis and processing of the representative semiconducting alternating copolymer poly(9,9-dioctylfluorene-*alt*-bithiophene) (PF8T2) in high yield and high quality and with transistor performances comparable with those obtained with reference materials synthesized and processed from volatile organic solvents.

1. Introduction

Conjugated semiconducting polymers are key components for printed electronics, a field rapidly approaching the laboratory to industry transition. Over the last few decades, enormous progresses in the development of reliable structure properties relationships enabled the synthesis of very efficient active materials for organic light emitting devices (OLEDs),^[1] organic photovoltaic (OPV) cells,^[2] organic field effect transistors (OFETs),^[3] thermoelectric generators,^[4,5] chemical sensors,^[6] bioelectronic devices,^[7] light emitting electrochemical cells,^[8] electrochromic devices,^[9,10] and many more. The main reasons for the success of this class of materials are the vast tunability of properties that can be achieved through molecular design and the processability via wet techniques. The emphasis on the possibility to process such materials almost completely through solvent-based printing

techniques is a particularly attractive feature in terms of cost reduction and compatibility with a large variety of substrates, including food^[11] and even the human skin.^[12]


So far, the research focused prevalently on performances so that the minimum requirements for the proof-of-concept validation of the different technologies could be fulfilled. More recently, the consolidated performances demonstrated in OLEDs, organic thin film transistors (OTFTs) and OPV cells urged researchers to include sustainability and costing into the big picture of the Lab to Fab transition.^[13] Indeed, materials having an overcomplex synthesis are bound to be too expensive to make a convincing case.^[14] Also, organic synthesis is very heavily relying on the use of volatile organic compounds (VOCs), raising increasing environmental concerns.

With the notable exception of the well-established poly-3-hexylthiophene, and of the recently introduced polymers obtained by aldol polycondensation of phenyl-bis-oxindole and phenyl-bis-isatin monomers,^[15] semiconducting polymers (and copolymers) are prepared via C–C cross coupling reactions, preferentially according to Stille and Suzuki–Miyaura (SM) protocols. The Stille reaction generally affords higher molecular weights

C. Ceriani, S. Mattiello, M. Sassi, N. Pianta, L. Beverina
Department of Materials Science
University of Milano-Bicocca and INSTM
Via R. Cozzi, 55, Milan I-20125, Italy
E-mail: luca.beverina@unimib.it

M. Scagliotti, M. Rapisarda, L. Mariucci
CNR-IMM
Via del Fosso del Cavaliere 100, Rome 00133, Italy
E-mail: matteo.rapisarda@cnr.it

T. Losi, A. Luzio, M. Caironi
Center for Nano Science and Technology@PoliMi
Istituto Italiano di Tecnologia
Via Giovanni Pascoli 70/3, Milan 20133, Italy
E-mail: mario.caironi@iit.it

 The ORCID identification number(s) for the author(s) of this article can be found under <https://doi.org/10.1002/aelm.202201160>.

© 2023 The Authors. Advanced Electronic Materials published by Wiley-VCH GmbH. This is an open access article under the terms of the Creative Commons Attribution License, which permits use, distribution and reproduction in any medium, provided the original work is properly cited.

DOI: 10.1002/aelm.202201160

and small dispersity but is flawed by the production of highly toxic organotin compounds in stoichiometric amount with respect to one of the comonomers. The SM protocol does not produce intrinsically toxic species but is generally less efficient in providing high molecular weights and requires prolonged heating in solutions of organic solvents. The recently introduced direct arylation polymerization (DAP) represents a vast improvement in atom economy and enables a reduction in the number of synthetic steps, ultimately connected with the cost.^[16–22] On the downside, the method is not yet as general as the Stille coupling; reaction conditions require a careful optimization that is very much substrate dependent and prolonged heating in high boiling solvents of considerable toxicity.^[23] Electrochemical polymerization does not require the pre-activation of one of the monomers and offers ample control over reactions conditions, but is limited to the direct growth of the materials over a conductive substrate.^[24–27]

Aside from synthesis, all polymers require a solvent intensive purification consisting in prolonged washing with solvents of different polarity to remove impurities, side products, and to refine the molecular weight distribution.

Processing is no less problematic. Unless a specific molecular design heavily impacting on synthesis is implemented,^[28,29] semiconducting polymers are water insoluble. Toxic halogenated solvents like dichlorobenzene are still the standard in the field as they allow reaching the required concentrations and degree of self-assembly promoted preorganization of polymeric materials leading to best results in terms of film quality and morphology. To sum it up, while new materials with improved performances are almost daily reported, efforts on the improvement of sustainability and reduction of costs are comparatively less impressive.

Formulation chemistry provides the tool to use water as the processing solvent, even for strongly hydrophobic materials.^[30,31] The slow addition of a solution of a semiconducting polymer in a suitable water miscible organic solvent to a water solution of surfactants, leads to the formation of a colloidal dispersions of polymer nanoparticles in water.^[32] The organic solvent introduced can be removed by evaporation after the formation of the nanoparticles. Direct miniemulsion polymerization in the form of nanoparticles is also possible.^[33,34] The strategy was successful in the preparation of OFETs, OPV devices, and OLEDs exclusively from aqueous inks. The surfactants can also be chemically incorporated in the structure of the polymer thus enabling direct self-assembly in nanoparticles of the correct size.^[35,36] In all such approaches, the organic solvent is not present in the final ink, but it is still required during the preparation.

Recently the group of Turner reported a very promising new strategy, dramatically reducing reliance to organic solvents in both synthesis and processing.^[37] The strategy is based on two key ideas: the use of miniemulsion as the polymerization technique and of dialysis in water as the purification tool. In miniemulsion polymerization, reactions are performed in a biphasic mixture constituted by very small, surfactant stabilized droplets of an organic solvent within a water solution of a surfactant.^[38,39] The authors demonstrated that the approach provides a remarkable control over dimensions and shape of the polymer nanoparticles thus obtained. Such surfactant stabilized

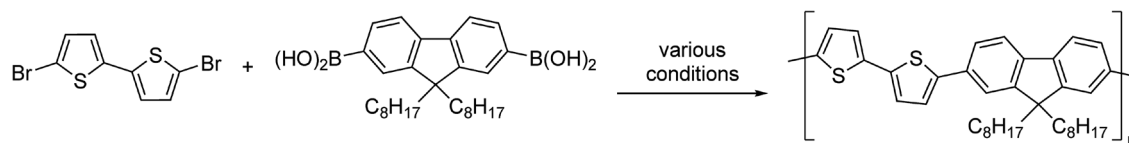
nanoparticles can be purified from water soluble by-products and excess surfactant by inexpensive and organic solvent free dialysis, leading to an aqueous ink that could be used directly for processing. The authors demonstrated that efficient devices can be obtained, provided that the active layer is rinsed with ethanol after deposition to further remove impurities. The approach represents a very dramatic improvement toward sustainability and cost reduction.

Inspired, we recently demonstrated that micellar chemistry could help pushing sustainability in organic semiconductors even further, to the point of completely removing the need for toxic organic solvents at all stages. The core concept of the micellar catalysis approach is the capability of selected surfactants to assemble in water solution into association colloids featuring lipophilic pockets where hydrophobic derivatives can be hosted, thereby efficiently reacting due to the high local concentration.^[40] Reactions are fast, require only moderate heating and enable a dramatic reduction in the amount of catalyst required.^[41–47] The approach is different from the miniemulsion polymerization as no organic solvent is required. The field of micellar catalysis is rapidly evolving toward widespread application in process chemistry with notable examples of large scale synthesis of active pharmaceutical ingredients (API).^[48–50] Micellar catalysis is rapidly becoming a resourceful tool for the synthesis of organic semiconductors for printable (opto)electronics as well.^[51–55]

The detailed nature of the colloidal state better describing a micellar catalyzed reaction at any given time very much depends on the surfactant employed, the physical state of reagents, products, and the presence of additives.^[56,57] The use of very small amounts of selected organic solvents generally improves results whenever reproducibility become relevant issue.^[58] We recently exploited the same approach in the first example of micellar catalyzed polymerization of a semiconducting material.^[53] We obtained competitive results only when using very small amounts of toluene. We later demonstrated that the use of a mixture of food grade lecithin and of the industrial surfactant Tween 80 represents an alternative and resourceful strategy to improve reproducibility without the need for organic solvents.^[57]

The Tween 80/L- α -lecithin 8:2 w:w mixture at 2 wt% in water (TL82) is a well-known emulsifier capable to readily provide finely dispersed emulsion of the most difficult to handle hydrophobic materials—including accidental oil spills over the sea—with a remarkable insensitivity to experimental set up and scale.^[59–61] The use of the TL82 mixture gave satisfactory results not only with the emulsions formed by liquid reagents but also with poorly soluble solids. Indeed, we demonstrated that almost insoluble halogenated organic pigments can be efficiently coupled with a variety of boronic acids while dispersed in a TL82 aqueous mixture.^[62] We here show that TL82 can be successfully used for the preparation of high molecular weight semiconducting polymers, where conversion of the growing oligomers in insoluble solids is expected to happen. The reaction is more efficient and purification becomes straightforward thus further improving the appeal of the method. Due to the proof of concept nature of this contribution, we focused our attention to a well-established p-type polymer: poly(9,9-dioctylfluorene-*alt*-bithiophene) (PF8T2). Such material has a solid background in

Table 1. Reaction condition, molecular weight (M_n and M_w) and dispersity (\mathcal{D}) for the synthesis of PF8T2. For Entry 1 Pd(PPh₃)₄ and NaOH were used. For Entry 2–6 Pd(dtbpf)Cl₂ and Et₃N.



Entry	Medium	T [°C]	Atm	Yield [%]	M_n [kg mol ⁻¹]	M_w [kg mol ⁻¹]	\mathcal{D}
1	Toluene	90	N ₂	94	24.2	39.8	1.64
2	K-EL	25	air	70	15.9	26.3	1.65
3	K-EL/Tol 9:1	80	air	87	25.2	49.4	1.96
4	TL82	80	air	80	18.1	33.3	1.84
5	TL82/Tol 9:1	80	air	60	18.2	29.7	1.63
6	TL82	80	N ₂	76	16.1	28.5	1.77

printed electronics and possesses well known semiconducting features making the comparison of our results with literature data more straightforward. Nowadays it is seldom used for state of the art devices due to a relatively poor mobility, yet the results we here describe are general and will be extended to higher performance materials in the future. Finally, we demonstrate the fabrication of OFET devices using aqueous inks and having performances comparable with those obtained by the use of VOCs in both synthesis and processing.

2. Results and Discussion

2.1. Polymerization Reactions and Purification Protocols

Recently, we demonstrated that two well established polymers having documented application in printed electronics—PF8T2 and poly(9,9-dioctylfluorene-*alt*-benzothiadiazole) (PF8BT)—can be efficiently prepared via micellar SM in water.^[63] The optimization of the reaction conditions required the introduction of a small amount of toluene to prevent massive phase segregation as the molecular weights increased. The protocol represents an improvement over literature as it requires 0.2 L of toluene for every mol of monomer, to be compared with the 12.5 L required by miniemulsion.^[37] It should be stressed that the role of toluene in the two approaches is different, with consequences in the purification step. While working under miniemulsion conditions, every droplet of organic solvent is a microreactor where a nanoparticle of polymer is formed. In the case of micellar polymerizations, the amount of toluene is too small for the formation of droplets of oil phase. The polymerization happens in a complex mixture of reagents, surfactants (in our case the high molecular weight, branched industrial surfactant Kolliphor EL, K-EL),^[64] and toluene. Under such conditions, part of the surfactant can remain entangled in the growing conjugated polymer, negatively impacting on purification.

The presence of lecithin in TL82 makes it possible to completely remove the toluene. We have recently shown that lecithin gives homogeneous dispersion of organic solids in water and makes it possible to efficiently carrying out SM reactions without dissolving the reagents.^[57,62] Under such conditions, the formation of an interpenetrating polymeric network would

be prevented as the solid monomers are never dissolved, but slowly etched at the surface by the action of the dispersant. Prior to proceed with the polymerization, we optimized the reaction conditions on small molecule model compounds—as discussed in Supporting Information—confirming that TL82 is at least as efficient as the previously employed mixture of K-EL 2 wt% in water in the presence of 10 vol% toluene.

We thus moved to the copolymerization of 9,9-dioctylfluorene-2,7-diboronic acid and 5,5'-dibromo-2,2'-bithiophene, which we performed in TL82, with NEt₃ as the base and a 4 mol% of [1,1'-bis(di-tert-butylphosphino)ferrocene] dichloropalladium(II) (Pd(dtbpf)Cl₂) as the catalyst. We also performed control experiments in organic solvent and in the previously employed micellar conditions. Results are summarized in **Table 1**.

Performing the reaction under standard, organic solvent promoted conditions (entry 1) and under micellar catalysis with K-EL in the presence of 10 vol% of toluene (entry 3) gives essentially the same results in terms of yield and molecular weight. K-EL alone (entry 2) gives lower yield and shorter polymers. In our previous paper we analyzed the effect in detail.^[63] The use of the TL82 formulation both under standard laboratory atmosphere (entry 4) and under N₂ (entry 6) gives comparable results that are intermediate in terms of yield and molecular weight between the case of K-EL and the control reaction in plain toluene. The use of toluene as the co-solvent (entry 5) does not improve polymerization statistics and slightly reduces yield. The results agree with our previous experience with the TL82 mixture.^[57]

All polymers were purified according to the same protocol—filtration of the crude and successive Soxhlet extractions with MeOH, acetone, heptane, and chloroform—characterized in terms of molecular weight and used for the preparation of devices as outlined in the next section. All yields reported are after Soxhlet purification.

Figure 1 shows the comparison of the ¹H NMR spectra of Entries 1, 3, and 4 samples. While the dispersion polymerized and reference materials display the same peaks, the spectrum of the micellar polymerized sample contains extra peaks in the aliphatic region that can be assigned to traces of K-EL. Indeed, in the case of the formation of a colloidal interpenetrating polymer network, the solvent extraction protocol is not expected to be fully efficient in removing residual surfactant.

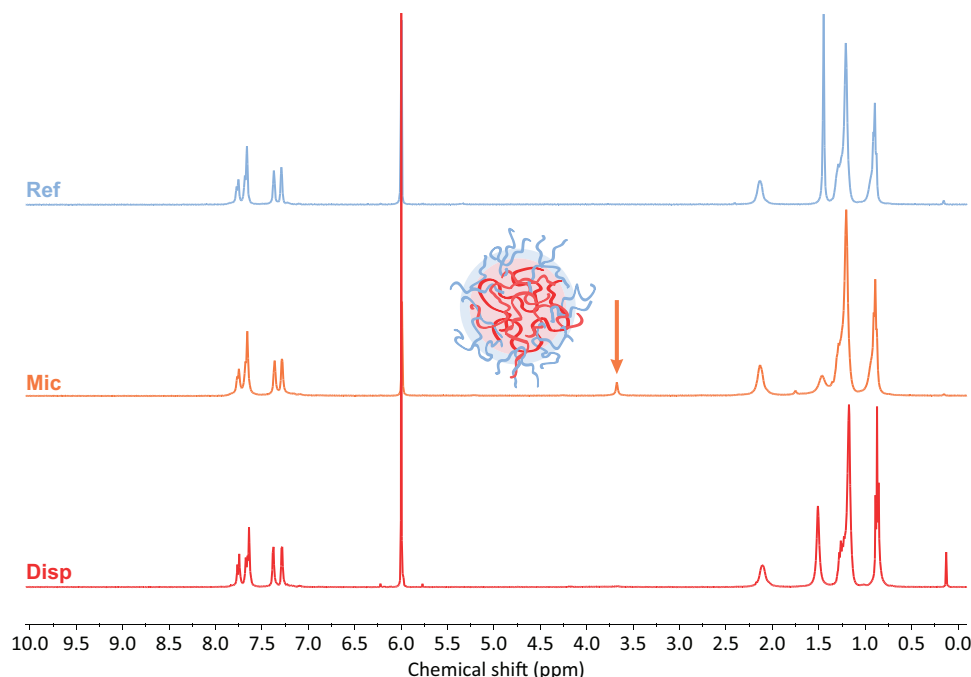


Figure 1. Comparison between the ^1H NMR spectra of the Ref (blue), Mic (orange), and Disp (red) samples of PF8T2 in $\text{C}_2\text{D}_2\text{Cl}_4$ at 353 K. The arrow highlights the extra peak corresponding to the interpenetrating residual surfactant. The cartoon close to the extra peak is a representation of an interpenetrating polymeric network between the surfactant (blue) and the PF8T2 (red).

A portion of the sample we obtained according to the procedure described in entry 3 was further purified by dissolution in the minimum amount of THF, reprecipitation in water followed by probe sonication and recovery via centrifugation. By NMR analysis, the procedure reduced the amount of residual surfactant, without completely removing it (see also Figures S7, S8, Supporting Information). Conversely, no extra peaks are present in the NMR of the sample polymerized in TL82, thus confirming that in the case of dispersion polymerization the surfactant do not contaminate the product. We characterized the Disp sample electrochemically via impedance spectroscopy (Figure S9, Supporting Information), cyclic and differential pulsed voltammetry (Figure S10, Supporting Information).

2.2. Organic Solvent Processed Devices

To assess the impact of surfactant contamination in the PF8T2 samples polymerized according to the different routes described in the previous paragraph, we prepared OTFT devices with control sample (Table 1, entry 1 from now on identified as Ref), micellar polymerized sample (Table 1, entry 3 from now on identified as Mic sample), of the Mic sample further purified by reprecipitation and probe sonication (from now on identified as Mic-P sample) and of the dispersion polymerized sample (Table 1, entry 4 sample, from now on identified as Disp sample). The scope of this first battery of devices is the comparison, under otherwise identical experimental conditions, of the quality of materials obtained via the different polymerization techniques. All materials received the same purification protocol (aside from Mic-P that was subjected to an additional step) and were processed using organic solvents.

As it is thoroughly discussed in the ESI section, we considered three different transistor configurations aiming at matching literature performances for the Ref sample: Bottom gate bottom contact with SiO_2 as the dielectric (BGBC), bottom gate top contact with SiO_2 as the dielectric (BGTC SiO_2), and bottom gate top contact with SiO_2 and PMMA in series as the dielectric (BGTC PMMA). **Figure 2a** shows that the BGTC PMMA configuration gave the best device characteristics in terms of hysteresis, on-off ratio (exceeding 10^3) and field-effect saturation mobility (μ of about $0.5 \times 10^{-3} \text{ cm}^2 \text{ V}^{-1} \text{ s}^{-1}$). We thus tested Mic, Mic-P, and Disp samples using the BGTC PMMA (from now on simply BGTC) configuration.

Figure 2b,c shows the typical transfer characteristics of the BGTC devices we obtained with the Mic samples, without and with rinsing the polymer film with EtOH. This post deposition step enables the removal of excess surfactant possibly contaminating the sample and generally improves performances.^[37] In our case, the rinsing only marginally affected the performances, raising the mobility from 1.9 to $4.6 \times 10^{-5} \text{ cm}^2 \text{ V}^{-1} \text{ s}^{-1}$. An appreciable hysteresis, insensitive to the ethanol bath, affected the transfer curves of both samples. Performances improved significantly while characterizing the purified Mic-P sample. **Figure 3a** shows that the hysteresis in the transfer plot is significantly reduced and more closely matches that of the Ref sample. We measured a field-effect saturation mobility of $2.4 \times 10^{-4} \text{ cm}^2 \text{ V}^{-1} \text{ s}^{-1}$, which is five times larger than that of the EtOH rinsed sample, yet still half that of the Ref sample. **Figure 3b** shows the output characteristics of the Mic-P device, highlighting a good linearity at low V_{DS} and a flat saturation region. Such characteristics suggest a good quality of the semiconductor/dielectric interface, a low defect density in the organic semiconductor layer, and a good coupling between the metal

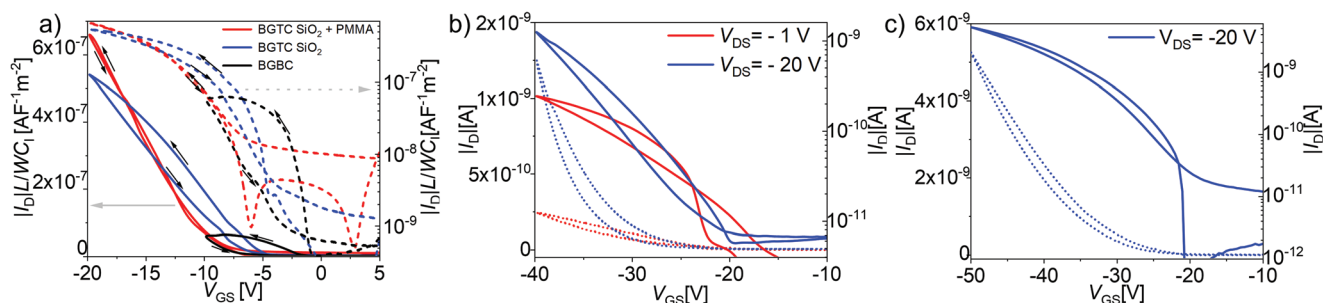


Figure 2. a) Comparison of the normalized up-down transfer characteristics with $V_{DS} = -20$ V of devices, based on Ref sample and having the three different structures we tested. b) Up-down transfer characteristics of a BGTC PMMA devices with Mic sample measured in linear ($V_{DS} = -1$ V, red lines) and saturated regime ($V_{DS} = -20$ V, blue lines) The dotted lines refer to linear left scale and the continuous lines refer to right log scale. The black arrows indicate the direction (up or down) of $I-V$ acquisition. c) Up-down transfer characteristic with $V_{DS} = -20$ V of a BGTC PMMA devices with EtOH- washed Mic sample. The dotted lines refer to linear left scale and the continuous lines refer to right log scale. The black arrows indicate the direction (up or down) of $I-V$ acquisition.

work-function of gold electrodes and the energy bands of the semiconductor, as evidenced by the linearity of the output characteristics at low V_{DS} that suggests a negligible contact resistance. Figure 3c shows the non-contact mode atomic force microscopy (AFM) 2×2 μm topographic image of the Mic-P semiconductor layers. The film thickness is 25 nm and its top surface appears composed by structures with lateral dimensions of a several hundred nm well connected to each other. The surface corrugation is low, the calculated RMS roughness is (0.7 ± 0.2) nm. The NMR analysis shows that not even the very thorough washing under probe sonication in a hydro/alcoholic solution is efficient in completely removing the entrapped

surfactant, which could explain the small discrepancy in the saturation mobility.

We then moved to the characterization of the Disp samples. Figure 3d,e shows that the transfer characteristics and I_D versus V_{DS} output characteristics of the Disp sample devices are very much in line with those of the EtOH rinsed Mic-P samples, even showing the improved field-effect saturation mobility of 3.5×10^{-4} $\text{cm}^2 \text{V}^{-1} \text{s}^{-1}$. This value is very close to the one obtained with the Ref compound measured under identical experimental conditions. As already discussed, the reference polymer has a slightly higher molecular weight with respect to the Disp one, which could explain the smaller discrepancy.

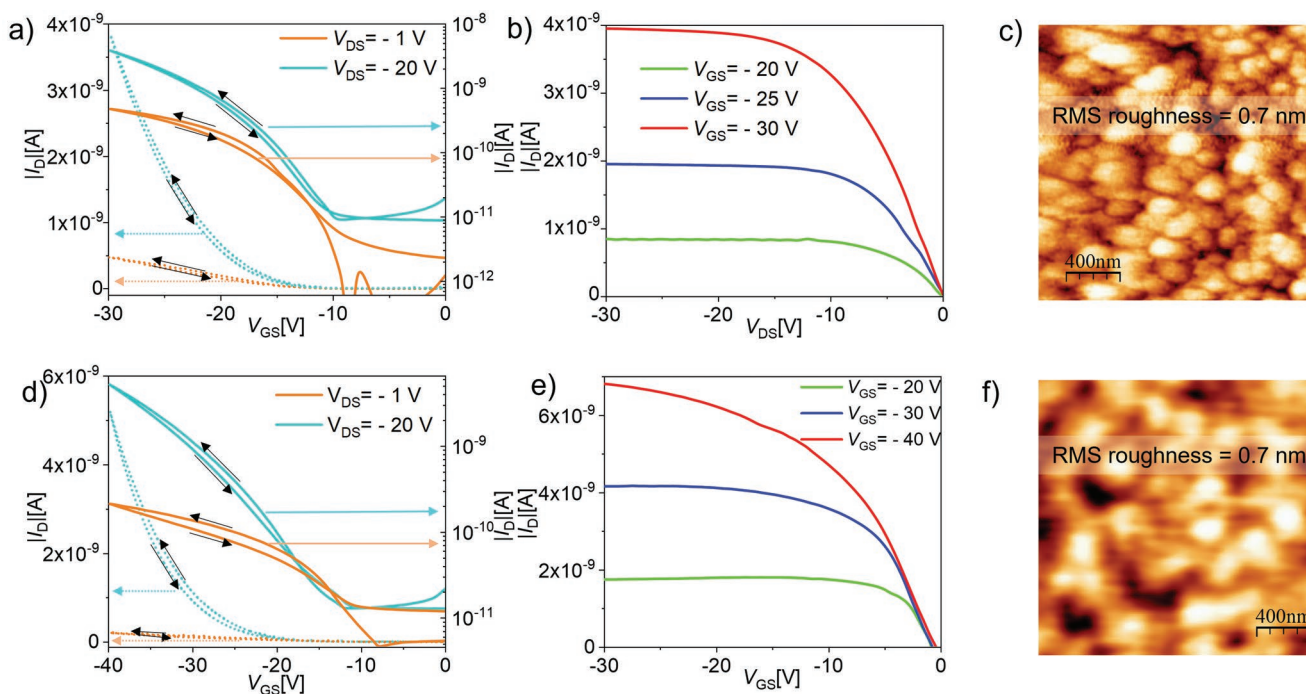


Figure 3. Up-down transfer characteristics of PMMA-BGTC OTFT devices measured in linear ($V_{DS} = -1$ V, orange lines) and saturated regime ($V_{DS} = -20$ V, blue lines) fabricated with a) Mic-P and d) Disp materials. The dotted lines refer to linear left scale and the continuous lines refer to right log scale. The black arrows indicate the direction (up or down) of $I-V$ acquisition. Output I_D versus V_{DS} characteristics of PMMA-BGTC OTFT devices fabricated with b) Mic-P and e) Disp materials for different values of V_{GS} . c, f) AFM topography 2×2 μm images of Mic-P and Disp OTFT top semiconductor surface, respectively.

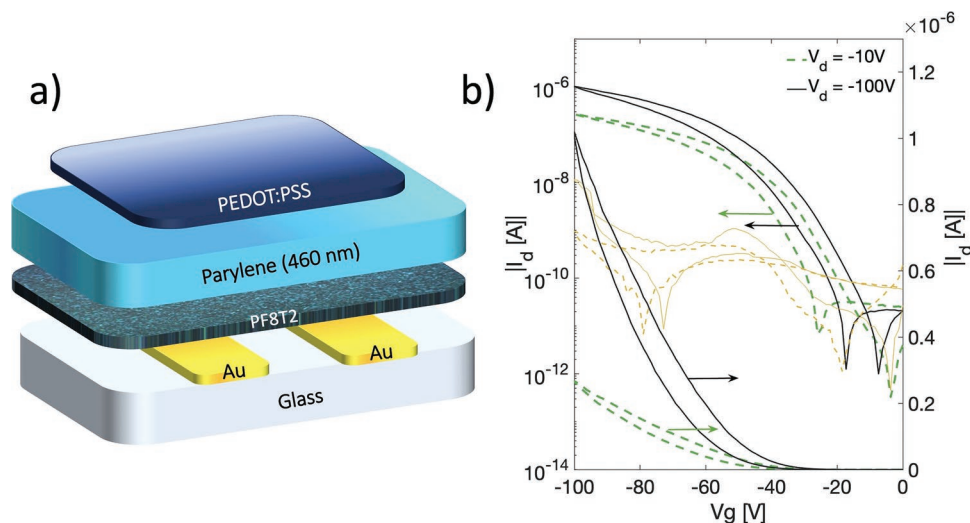


Figure 4. a) Device architecture of the water processed field-effect transistors with channel width (W) and channel length (L) of 2 mm and 20 μm . b) Representative transfer characteristic curve of the fabricated devices based on PF8T2 aqueous dispersion.

The AFM of the top semiconductor layer of Disp devices shown in Figure 3f does not show any meaningful difference with respect to that of Mic-P samples. It should be stressed that, differently from the Mic-P samples, in the case of Disp devices we had no evidence of contamination from surfactants and thus we did not perform the ethanol rinse after the deposition from the CHCl_3 solution.

The values we obtained are generally low as state-of-the-art polymers feature mobility well above $1 \text{ cm}^2 \text{ V}^{-1} \text{ s}^{-1}$.^[3] Yet, the values we obtained for the different samples span over two orders of magnitude thus enabling to draw conclusion in terms of process-performances relationships.

2.3. Aqueous Ink Processed Devices

Having validated the dispersion approach in terms of absolute performances of the materials, we tested the organic solvent free protocol previously described by Turner to achieve a completely organic solvent free synthesis and processing approach.^[37] Thus, we performed the polymerization reaction under conditions identical with respect to those employed for the Disp samples. At the end of the polymerization, we transferred the mixture (a viscous deeply orange colored suspension) into a dialysis cassette (2 kDa MWCO), immersed it in DI water and left it to stir over a period of 72 h. We replaced the DI water every 24 h. We finally recovered the purified mixture, and we diluted it to reach a concentration of about 0.025 M with respect to the repeating unit. At such a concentration, the mixture can be used directly for device fabrication. We intentionally did not perform any other purification as such this sample cannot be purer than the Dips one described in the previous section.

The use of an aqueous ink required a slightly different device structure, mostly due to the poor wettability of PMMA by water. Thus, we fabricated TGBC field-effect transistors on glass substrates. Gold contacts for source and drain electrodes were patterned by standard photolithography. The substrates were treated by oxygen plasma to make the surface hydrophilic and

increase wettability by the aqueous ink. After that, the aqueous dispersion of PF8T2 was filtered (0.2 μm syringe filter) and then deposited by spin-coating. The films were successively heated at 150 $^\circ\text{C}$ for 30 min to completely remove traces of water and washed in ethanol to remove excess surfactant. Finally, a 460 nm thick parylene-C layer was deposited by chemical vapor deposition and then a PEDOT:PSS gate was inject printed to complete the devices. **Figure 4a)** shows a sketch of the transistors structure, while in **Figure 4b)** a representative characteristic transfer curve in both linear and saturation regime is presented.

We measured a field-effect mobility as high as 1.2×10^{-3} and $1 \times 10^{-3} \text{ cm}^2 \text{ V}^{-1} \text{ s}^{-1}$ for linear ($V_{\text{DS}} = 10 \text{ V}$) and saturation ($V_{\text{DS}} = 100 \text{ V}$) regime respectively, which are perfectly comparable with organic solvent processed Ref devices described in Section 2.2, confirming the efficacy of the approach. However, differently from the latter, an appreciable hysteresis is present and could not be eliminated even after a washing step. The marked hysteresis cycle along with the high threshold voltages ($V_{\text{TH lin}} = -45 \text{ V}$, $V_{\text{TH sat}} = -30 \text{ V}$) and a non-ideal extended sub-threshold region are indications of the presence of shallow traps, possibly due to polymerization defects and/or terminations. We are actively working at the further optimization of the procedure. The characterization of device stability will also be the subject of further studies.

3. Conclusion

We have demonstrated that the use of an aqueous solutions of a specific mixture of an industrial surfactant (Tween 80) and a food grade additive (lecithin) enables to efficiently perform the SM polymerization of the p-type polymer PF8T2 in the absence of any organic solvent. The protocol affords polymers having comparable polymerization statistics with respect to reference materials obtained in organic solvents and is advantageous in terms of overall sustainability and purity of the final materials. We compared the new protocol with previously developed

micellar approaches, demonstrating that the dispersion technique enables a much more straightforward purification from processing additives. The influence of such impurities was thoroughly evaluated using OFETs as testbed for the transport properties of the different samples prepared according to organic solvent, micellar, and dispersion polymerization. Finally, we adapted a literature procedure for the polymerization and dialysis purification of water dispersion of conjugated polymers nanoaggregates to our dispersion approach. We successfully produced a directly printable aqueous ink of PF8T2 starting from the corresponding monomers without recurring to the use of organic solvents at all steps, including purification and film deposition. The water processed devices gave a saturation mobility for holes of $1 \times 10^{-3} \text{ cm}^2 \text{ V}^{-1} \text{ s}^{-1}$, a value in line with the best reported ones for organic solvent synthesized and processed PF8T2 samples having comparable polymerization statistics. Work is in progress to extend the approach to higher mobility polymers.

4. Experimental Section

General Procedure for Model Reactions in Surfactant Solution: All reactions were carried out in a 5 mL CEM microwave glass tube vial under magnetic stirring at 800 rpm and at a nominal concentration for fluorene derivative of 0.5 mol L^{-1} . Depending on the experiment, the reaction medium the temperature and the atmosphere were studied (See Table S1, Supporting Information).

9,9-dioctylfluorene-2,7-diboronic acid (119 mg, 0.25 mmol), 2-bromothiophene acid (81.5 mg, 0.50 mmol), and Pd(dtbpf)Cl₂ (6.5 mg, 0.01 mmol) were weighed in the vial and then reaction medium was added. The mixture was stirred and allowed to homogenize for 5 min before addition of the NEt₃ (152 mg, 1.50 mmol). All reactions were stopped after 12 h of stirring at the chosen temperature, extracted with CH₂Cl₂, filtered over a pad of silica gel, and submitted to GC-MS characterization.

Polymerization of PF8T2 in Surfactant Solution, General Procedure: All the polymerizations were carried out in a 5 mL CEM microwave glass tube vial under magnetic stirring at 800 rpm and at a nominal concentration for the monomers of 0.25 mol L^{-1} . Depending on the experiment, the medium varied (see Table 1).

A representative experimental procedure is given as an example: 9,9-dioctylfluorene-2,7 diboronic acid (239 mg, 0.5 mmol), 5,5'-dibromo-2,2'-bithiophene (162 mg, 0.5 mmol), and Pd(dtbpf)Cl₂ (13.0 mg, 0.02 mmol) were weighed in the vial and then 2 mL of surfactant/s 2 wt% in water was added. The mixture was stirred and allowed to homogenize for 5 min at 80 °C, heating with an oil bath, before addition of the NEt₃ (304 mg, 3.0 mmol). After the addition of the base, the reaction mixture was stirred at 80 °C for 48 h. To provide defined end-groups, phenylboronic acid (183 mg, 1.5 mmol), and after 2 h bromobenzene (157 mg, 1.5 mmol) were added. After stirring for further 2 h the polymer was precipitated in methanol (10 mL) and then submitted to Soxhlet extraction with MeOH, acetone, heptane, and chloroform to remove the excess of end-capping agents, catalyst residues, and oligomers.

PF8T2 Aqueous Ink: 9,9-Dioctylfluorene-2,7-diboronic acid (239 mg, 0.5 mmol), 5,5'-dibromo-2,2'-bithiophene (162 mg, 0.5 mmol), and Pd(dtbpf)Cl₂ (13.0 mg, 0.02 mmol) were weighed in the vial and then 2 mL of TL82 mixture 2 wt% in water was added. The mixture was stirred and allowed to homogenize for 5 min at 80 °C, heating with an oil bath, before addition of the NEt₃ (304 mg, 3.0 mmol).

After the addition of the base, the reaction mixture was stirred at 80 °C for 48 h. After cooling, the dispersion was injected into a Thermo Scientific Slide-A-Lyzer dialysis cassette (2 kDa MWCO), immersed in DI water, and left to stir over a period of 72 h. The DI water was replaced

every 12 h. After dialysis, the dispersion was diluted to a concentration of 0.025 M with 18 mL of DI water. The resulting dispersion was used for further characterization and processing into thin-films.

Assembly and Characterization of the Devices: Organic Solvent Processed Devices Fabrication: All organic semiconductor solutions were stirred at room temperature for 24 h under nitrogen atmosphere and prior to deposition they were heated at 60 °C for 30 min. For both BGBC and BGTC structures (Figures 2a and 2b, respectively) the gate (G) is formed by a heavily doped Si wafer plus 100 nm of SiO₂ acting as gate dielectric. Then in BGBC devices, the source (S) and drain (D) Au contacts (25 nm thickness) were thermally evaporated in vacuum with a deposition rate of 1 nm s^{-1} and patterned using the Lift-off lithographic technique. Before Au evaporation, the SiO₂ surface was treated with HMDS to promote Au adhesion with SiO₂. We then deposited the active material by spin coating at 1500 rpm for 30 s, followed by annealing at 110 °C for 10 min. The obtained semiconductor film thickness was 30 nm measured by a profilometer. The as-devised BGBC structure had semiconductor channel length $L = 100 \mu\text{m}$ and channel width $W = 200 \mu\text{m}$. In BGTC devices the organic semiconductor was deposited directly on the dielectric layer and subsequently by using a shadow mask (AISI 304 stainless steel, 50 μm thick, Stencils Unlimited) to evaporate the Au S&D contacts ($L = 100 \mu\text{m}$ and $W = 1000 \mu\text{m}$) directly on top of the semiconductor material (Figure 2b). As discussed in results section, in specific cases a 300-nm layer of PMMA was also introduced on top of SiO₂ layer to improve the quality of the semiconducting layer. Besides, the staggered BGTC configuration was suitable to reduce contact effects and therefore focus and analyze the properties of the organic semiconductor layer.^[3,4] The whole fabrication process, carried out in cleanroom environment at low temperature (<150 °C), was compatible with a large area flexible organic electronics^[5,6] and allowed a fast, simple, and clean process.^[7]

Devices Electrical Characterization: The organic solved processed devices have been electrically characterized in an MMR cryostat using a Keithley 236 source/measure unit and a Keithley 2635 source/meter.

Aqueous Ink Processed Devices Fabrication: Then bottom source and drain electrodes were patterned by standard photolithography on glass substrates (low alkali 1737F Corning glasses, purchased from Präzisions Glas & Optik GmbH) and deposited by thermal evaporation: 35 nm thick Au with a 3 nm thick Cr adhesion layer. The substrates were then cleaned by sonication with acetone and isopropyl alcohol (both purchased from Sigma-Aldrich) for 10 and 5 min. Afterward an oxygen plasma treatment was performed (5 min at 100 W). Then the filtered (0.2 μm syringe filter) aqueous dispersion of the semiconducting polymer PF8T2 was deposited by spin-coating (500 rpm for 60 s, 4000 rpm for 10 s). After active layer deposition, the devices were heated up at 150 °C for 30 min and successively washed in ethanol to remove a possible excess of surfactant. Then, a 470 nm thick layer of Parylene-C (dimer purchased from Specialty Coating Systems) was deposited by CVD with an SCS Labcoater 2-PDS2010 system. To complete the devices PEDOT:PSS (Clevios PJ700 formulation, purchased from Heraeus) gate electrodes were inkjet printed with of Fujifilm Dimatix DMP2831 at room temperature.

The aqueous ink processed devices were measured with semiconductor parameter analyzer (Agilent B1500A) inside a glove box with a Wentworth Laboratories probe station.

Supporting Information

Supporting Information is available from the Wiley Online Library or from the author.

Acknowledgements

This work was supported by MIUR under 2017YXX8AZ PRIN grant. M.C. and A.L. acknowledge support by the European Research Council

(ERC) under the European Union Horizon 2020 research and innovation program “ELFO,” grant agreement 864299, by the European Union H2020-EU.4.b. Twinning of research institutions “GREENELIT,” grant agreement 951747, and by the Sustainability Activity of Istituto Italiano di Tecnologia. The fabrication of the devices was partially carried out at PoliFab, the micro and nanotechnology center of the Politecnico di Milano. A mistake in the affiliations for M.S. was rectified after initial online publication, in May 2023.

Conflict of Interest

The authors declare no conflict of interest.

Data Availability Statement

The data that support the findings of this study are available in the supplementary material of this article.

Keywords

conjugated polymers, dispersion polymerization, micellar catalysis, organic field effect transistors, processing from water, sustainability

Received: October 18, 2022

Revised: January 19, 2023

Published online: March 21, 2023

- [1] J.-X. Chen, Y.-F. Xiao, K. Wang, D. Sun, X.-C. Fan, X. Zhang, M. Zhang, Y.-Z. Shi, J. Yu, F.-X. Geng, C.-S. Lee, X.-H. Zhang, *Angew. Chem., Int. Ed.* **2021**, *60*, 2478.
- [2] J. Hou, O. Inganäs, R. H. Friend, F. Gao, *Nat. Mater.* **2018**, *17*, 119.
- [3] A. F. Paterson, S. Singh, K. J. Fallon, T. Hodsdon, Y. Han, B. C. Schroeder, H. Bronstein, M. Heeney, I. McCulloch, T. D. Anthopoulos, *Adv. Mater.* **2018**, *30*, 1801079.
- [4] Q. Jiang, H. Sun, D. Zhao, F. Zhang, D. Hu, F. Jiao, L. Qin, V. Linseis, S. Fabiano, X. Crispin, Y. Ma, Y. Cao, *Adv. Mater.* **2020**, *32*, 2002752.
- [5] D. Kiefer, A. Giovannitti, H. Sun, T. Biskup, A. Hofmann, M. Koopmans, C. Cendra, S. Weber, L. J. Anton Koster, E. Olsson, J. Rivnay, S. Fabiano, I. McCulloch, C. Müller, *ACS Energy Lett.* **2018**, *3*, 278.
- [6] C. Deraedt, A. Rapakousiou, Y. Wang, L. Salmon, M. Bousquet, D. Astruc, *Angew. Chem., Int. Ed.* **2014**, *53*, 8445.
- [7] M. Magliulo, M. Y. Mulla, M. Singh, E. Macchia, A. Tiwari, L. Torsi, K. Manoli, *Pr. Kom. Mat.-Przyr., Poznan. Tow. Przyj. Nauk, Pr. Chem.* **2015**, *3*, 12347.
- [8] E. Fresta, R. D. Costa, *Pr. Kom. Mat.-Przyr., Poznan. Tow. Przyj. Nauk, Pr. Chem.* **2017**, *5*, 5643.
- [9] S. Macher, M. Schott, M. Sassi, I. Facchinetti, R. Ruffo, G. Patriarca, L. Beverina, U. Posset, G. A. Giffin, P. Löbmann, *Adv. Funct. Mater.* **2020**, *30*, 1906254.
- [10] S. Macher, M. Sassi, L. Beverina, U. Posset, M. Schott, G. A. Giffin, P. Löbmann, *ChemElectroChem* **2021**, *8*, 726.
- [11] A. S. Sharova, F. Melloni, G. Lanzani, C. J. Bettinger, M. Caironi, *Adv. Mater.* **2021**, *6*, 2000757.
- [12] G. E. Bonacchini, C. Bossio, F. Greco, V. Mattoli, Y.-H. Kim, G. Lanzani, M. Caironi, *Adv. Mater.* **2018**, *30*, 1706091.
- [13] R. Po, A. Bernardi, A. Calabrese, C. Carbonera, G. Corso, A. Pellegrino, *Energy Environ. Sci.* **2014**, *7*, 925.
- [14] R. Po, G. Bianchi, C. Carbonera, A. Pellegrino, *Macromolecules* **2015**, *48*, 453.
- [15] A. Onwubiko, W. Yue, C. Jellett, M. Xiao, H.-Y. Chen, M. K. Ravva, D. A. Hanifi, A.-C. Knall, B. Purushothaman, M. Nikolka, J.-C. Flores, A. Salleo, J.-L. Bredas, H. Sirringhaus, P. Hayoz, I. McCulloch, *Nat. Commun.* **2018**, *9*, 416.
- [16] A. Sanzone, S. Cimò, S. Mattiello, R. Ruffo, I. Facchinetti, G. Bonacchini, M. Caironi, M. Sassi, M. Sommer, L. Beverina, *ChemPlusChem* **2019**, *84*, 1346.
- [17] L. Ye, T. Hooshmand, B. C. Thompson, *Polym. Chem.* **2021**, *12*, 6688.
- [18] R. Matsidik, H. Komber, A. Luzio, M. Caironi, M. Sommer, *J. Am. Chem. Soc.* **2015**, *137*, 6705.
- [19] N. S. Gobalasingham, S. Noh, B. C. Thompson, *Polym. Chem.* **2016**, *7*, 1623.
- [20] A. S. Dudnik, T. J. Aldrich, N. D. Eastham, R. P. H. Chang, A. Facchetti, T. J. Marks, *J. Am. Chem. Soc.* **2016**, *138*, 15699.
- [21] A. Nitti, G. Bianchi, R. Po, T. M. Swager, D. Pasini, *J. Am. Chem. Soc.* **2017**, *139*, 8788.
- [22] A. Marrocchi, A. Facchetti, D. Lanari, C. Petrucci, L. Vaccaro, *Energy Environ. Sci.* **2016**, *9*, 763.
- [23] P.-O. Morin, T. Bura, B. Sun, S. I. Gorelsky, Y. Li, M. Leclerc, *ACS Macro Lett.* **2015**, *4*, 21.
- [24] R. M. G. Rajapakse, D. L. Watkins, T. A. Ranathunge, A. U. Malikaramage, H. M. N. P. Gunarathna, L. Sandakelum, S. Wylie, P. G. P. R. Abewardana, M. G. S. a. M. E. W. D. D. K. Egodawele, W. H. M. R. N. K. Herath, S. V. Bandara, D. R. Strongin, N. H. Attanayake, D. Velauthapillai, B. R. Horrocks, *RSC Adv.* **2022**, *12*, 12089.
- [25] R. M. G. Rajapakse, N. H. Attanayake, D. Karunathilaka, A. E. Steen, N. I. Hammer, D. R. Strongin, D. L. Watkins, *J. Mater. Chem. C* **2019**, *7*, 3168.
- [26] T. A. Ranathunge, D. T. Ngo, D. Karunathilaka, N. H. Attanayake, I. Chandrasiri, P. Brogdon, J. H. Delcamp, R. M. G. Rajapakse, D. L. Watkins, *J. Mater. Chem. C* **2020**, *8*, 5934.
- [27] N. E. Sparks, T. A. Ranathunge, N. H. Attanayake, P. Brogdon, J. H. Delcamp, R. M. G. Rajapakse, D. L. Watkins, *ChemElectroChem* **2020**, *7*, 3752.
- [28] Z. Hu, Z. Wang, X. Zhang, H. Tang, X. Liu, F. Huang, Y. Cao, *Science* **2019**, *13*, 33.
- [29] R. Kim, B. Kang, D. H. Sin, H. H. Choi, S.-K. Kwon, Y.-H. Kim, K. Cho, *Chem. Commun.* **2015**, *51*, 1524.
- [30] R. Breslow, *J. Phys. Org. Chem.* **2006**, *19*, 813.
- [31] B. H. Lipshutz, S. Ghorai, M. Cortes-Clerget, *Chem. - Eur. J.* **2018**, *24*, 6672.
- [32] Y. Jiang, J. McNeill, *Chem. Rev.* **2017**, *117*, 838.
- [33] J. M. Behrendt, J. A. Esquivel Guzman, L. Purdie, H. Willcock, J. J. Morrison, A. B. Foster, R. K. O'Reilly, M. C. McCairn, M. L. Turner, *React. Funct. Polym.* **2016**, *107*, 69.
- [34] D. Muenmart, A. B. Foster, A. Harvey, M.-T. Chen, O. Navarro, V. Promarak, M. C. McCairn, J. M. Behrendt, M. L. Turner, *Macromolecules* **2014**, *47*, 6531.
- [35] S. Zappia, G. Scavia, A. M. Ferretti, U. Giovannella, V. Vohra, S. Destri, *Adv. Sustainable Syst.* **2018**, *2*, 1700155.
- [36] S. Zappia, R. Mendichi, S. Battiato, G. Scavia, R. Mastria, F. Samperi, S. Destri, *Polymer* **2015**, *80*, 245.
- [37] A. Rahmanudin, R. Marcial-Hernandez, A. Zamhuri, A. S. Walton, D. J. Tate, R. U. Khan, S. Aphichatpanichakul, A. B. Foster, S. Broll, M. L. Turner, *Adv. Sci.* **2020**, *7*, 2002010.
- [38] J. Cho, S. Yoon, K. M. Sim, Y. J. Jeong, C. E. Park, S.-K. Kwon, Y.-H. Kim, D. S. Chung, *Energy Environ. Sci.* **2017**, *10*, 2324.
- [39] K. Landfester, *Adv. Mater.* **2001**, *13*, 765.
- [40] G. L. a. Sorella, G. Strukul, A. Scarso, *Green Chem.* **2015**, *17*, 644.
- [41] B. S. Takale, R. R. Thakore, F. Y. Kong, B. H. Lipshutz, *Green Chem.* **2019**, *21*, 6258.

- [42] B. S. Takale, R. R. Thakore, G. Casotti, X. Li, F. Gallou, B. H. Lipshutz, *Angew. Chem., Int. Ed.* **2021**, *60*, 4158.
- [43] R. R. Thakore, B. S. Takale, G. Casotti, E. S. Gao, H. S. Jin, B. H. Lipshutz, *Org. Lett.* **2020**, *22*, 6324.
- [44] X. Li, R. R. Thakore, B. S. Takale, F. Gallou, B. H. Lipshutz, *Org. Lett.* **2021**, *23*, 8114.
- [45] B. Jin, F. Gallou, J. Reilly, B. H. Lipshutz, *Chem. Sci.* **2019**, *10*, 3481.
- [46] S. Handa, B. Jin, P. P. Bora, Y. Wang, X. Zhang, F. Gallou, J. Reilly, B. H. Lipshutz, *ACS Catal.* **2019**, *9*, 2423.
- [47] Y. Zhang, B. S. Takale, F. Gallou, J. Reilly, B. H. Lipshutz, *Chem. Sci.* **2019**, *10*, 10556.
- [48] B. S. Takale, R. R. Thakore, R. Mallarapu, F. Gallou, B. H. Lipshutz, *Org. Process Res. Dev.* **2020**, *24*, 101.
- [49] M. Parmentier, M. Wagner, R. Wickendick, M. Baenziger, A. Langlois, F. Gallou, *Org. Process Res. Dev.* **2020**, *24*, 1536.
- [50] T.-Y. Yu, H. Pang, Y. Cao, F. Gallou, B. H. Lipshutz, *Angew. Chem., Int. Ed.* **2021**, *60*, 3708.
- [51] C. Ceriani, F. Corsini, G. Mattioli, S. Mattiello, D. Testa, R. Po, C. Botta, G. Griffini, L. Beverina, *J. Mater. Chem. C* **2021**, *9*, 14815.
- [52] M. Sassi, S. Mattiello, L. Beverina, *Eur. J. Org. Chem.* **2020**, *2020*, 3942.
- [53] A. Sanzone, S. Mattiello, G. M. Garavaglia, A. M. Calascibetta, C. Ceriani, M. Sassi, L. Beverina, *Green Chem.* **2019**, *21*, 4400.
- [54] A. Sanzone, A. Calascibetta, E. Ghiglietti, C. Ceriani, G. Mattioli, S. Mattiello, M. Sassi, L. Beverina, *J. Org. Chem.* **2018**, *83*, 15029.
- [55] S. Mattiello, M. Rooney, A. Sanzone, P. Brazzo, M. Sassi, L. Beverina, *Org. Lett.* **2017**, *19*, 654.
- [56] P. Hauk, J. Wencel-Delord, L. Ackermann, P. Walde, F. Gallou, *Curr. Opin. Colloid Interface Sci.* **2021**, *56*, 101506.
- [57] C. Ceriani, E. Ghiglietti, M. Sassi, S. Mattiello, L. Beverina, *Org. Process Res. Dev.* **2020**, *24*, 2604.
- [58] C. M. Gabriel, N. R. Lee, F. Bigorne, P. Klumphu, M. Parmentier, F. Gallou, B. H. Lipshutz, *Org. Lett.* **2016**, *19*, 194.
- [59] J. C. Athas, K. Jun, C. McCafferty, O. Owoseni, V. T. John, S. R. Raghavan, *Langmuir* **2014**, *30*, 9285.
- [60] D. A. Riehm, D. J. Rokke, P. G. Paul, H. S. Lee, B. S. Vizanko, A. V. McCormick, *J. Colloid Interface Sci.* **2017**, *487*, 52.
- [61] D. A. Riehm, J. E. Neilsen, G. D. Bothun, V. T. John, S. R. Raghavan, A. V. McCormick, *Mar. Pollut. Bull.* **2015**, *101*, 92.
- [62] C. Ceriani, F. Pallini, L. Mezzomo, M. Sassi, S. Mattiello, L. Beverina, *J. Organomet. Chem.* **2022**, *962*, 122267.
- [63] A. Sanzone, A. Calascibetta, M. Monti, S. Mattiello, M. Sassi, F. Corsini, G. Griffini, M. Sommer, L. Beverina, *ACS Macro Lett.* **2020**, *9*, 1167.
- [64] R. Ma, S.-Y. Chou, Y. Xie, Q. Pei, *Chem. Soc. Rev.* **2019**, *48*, 1741.